mathematics

MDPI

Article

Grey Wolf Optimizer for RES Capacity Factor Maximization at the Placement Planning Stage

Andrey M. Bramm *, Stanislav A. Eroshenko, Alexandra I. Khalyasmaa and Pavel V. Matrenin

Ural Power Engineering Institute, Ural Federal University Named after the First President of Russia B.N. Yeltsin, 620002 Ekaterinburg, Russia; s.a.eroshenko@urfu.ru (S.A.E.); a.i.khaliasmaa@urfu.ru (A.I.K.); p.v.matrenin@urfu.ru (P.V.M.)

* Correspondence: am.bramm@urfu.ru

Abstract: At the current stage of the integration of renewable energy sources into the power systems of many countries, requirements for compliance with established technical characteristics are being applied to power generation. One such requirement is the installed capacity utilization factor, which is extremely important for optimally placing power facilities based on renewable energy sources and for the successful development of renewable energy. Efficient placement maximizes the installed capacity utilization factor of a power facility, increasing energy efficiency and the payback period. The installed capacity utilization factor depends on the assumed meteorological factors relating to geographical location and the technical characteristics of power generation. However, the installed capacity utilization factor cannot be accurately predicted, since it is necessary to know the volume of electricity produced by the power facility. A novel approach to the optimization of placement of renewable energy source power plants and their capacity factor forecasting was proposed in this article. This approach combines a machine learning forecasting algorithm (random forest regressor) with a metaheuristic optimization algorithm (grey wolf optimizer). Although the proposed approach assumes the use of only open-source data, the simulations show better results than commonly used algorithms, such as random search, particle swarm optimizer, and firefly algorithm.

Keywords: capacity factor; forecasting; renewable energy sources; optimization; energy optimization; grey wolf optimizer

MSC: 68T20

Citation: Bramm, A.M.; Eroshenko, S.A.; Khalyasmaa, A.I.; Matrenin, P.V. Grey Wolf Optimizer for RES Capacity Factor Maximization at the Placement Planning Stage. *Mathematics* **2023**, *11*, 2545. https://doi.org/10.3390/math11112545

Academic Editors: Aspassia Daskalopulu, Dimitrios Bargiotas and Jinfeng Liu

Received: 22 April 2023
Revised: 13 May 2023
Accepted: 29 May 2023
Published: 1 June 2023

1. Introduction

Growth in the share of renewable energy sources (RES) in the generation profile will only intensify over the next five years against the backdrop of global energy development trends and strategies. According to the International Energy Agency (IEA) [1], from 2022 to 2027, 2400 GW of RES are planned. This capacity is equal to the total commissioning of RES for 2001–2021. At the same time, China, the European Union, the USA, and India plan to make the largest contribution to the increase in installed capacity. According to IEA forecasts, the capacity of new RES installations will be 1071.7 GW for China, 343.9 GW for the European Union, 280.6 GW for the USA, 145.6 GW for India, and about 329.5 GW for other countries.

Wind power plants (WPP) and photovoltaic power plants (PV) firmly dominate among new installed generation sources. Since 2019, WPPs and PVs account for more than 62% of all commissioning of generating capacities in the world energy industry [2] and more than 90% of generation commissioned based on RES.

The ever-increasing commissioning of installed RES capacity is aimed at reducing the carbon footprint. Reducing the carbon footprint in energy and industry is associated with minimizing the impact of human activities on climate change and global warming.

The global community has declared a 45% reduction in annual CO_2 emissions by 2030 and 70% by 2050 compared to today's emissions. The possibility of reducing CO_2 emissions by replacing carbon generation with RES has high potential [3]. The contribution of WPPs and PVs to carbon footprint reduction is estimated at 25–45% [4].

To achieve the declared performance, there are government support mechanisms for commissioning new RES. For the most part, measures of state support for RES consist of holding auctions for selecting projects that require the least capital investment. However, in order to provide such support, it is necessary to fulfill additional conditions regarding not only capital investment but also process performance, environmental impact, and other performance factors, depending on the auction [5].

Between January and September 2022, 77 GW of new RES capacity were selected worldwide. This is 70% higher than the commissioned competitive selection for 2021. RES auction capacities in 2022 in Europe increased by 60%. A record 11 GW of capacity was selected in the UK, with 3.5 GW each in France, Germany, and Italy.

As part of RES support programs in Commonwealth of Independent States (CIS) countries, minimum standards for the installed capacity utilization factor (*CF*) have been established [6]:

- 0.14—for solar generation power plants;
- 0.27—for wind generation power plants.

Power plants operating on the basis of solar and wind energy are not dispatchable, unlike thermal generation and hydro generation. For PVs and WPPs, it is only possible to limit output power. The generated power and electricity directly depend on climatic parameters and the availability of renewable resources in the territories where the power plants are located (the amount of solar radiation and wind speed). Renewable energy generation is a stochastic value, since the meteorological and climatic phenomena, on which it depends, are stochastic in nature [7,8].

Thus, when developing projects for commissioning new generating capacities with renewable energy sources, two main problems arise:

- forecasting the generation and installed capacity utilization factor of power plants with RES;
- choosing the optimal location for power plants with RES in order to maximize the installed capacity utilization factor.

The installed capacity utilization factor (*CF*) is a characteristic of the efficiency of renewable energy generation and is determined in accordance with the following expression:

$$CF = \frac{W_T}{P_{inst} \cdot T}, \quad (1)$$

where W_T is the amount of electricity produced at the generation plant with RES over time T; P_{inst} is the installed RES capacity of a power plant; and T is the period of time under consideration.

When using the classical expression (1) to determine the installed *CF*, it is assumed that the power plant is already operating or can undertake dispatchable power generation (when generation can be changed within a certain range in two directions). It is obvious that when calculating the RES installed capacity utilization factor, the value will stochastically change according to climatic and meteorological conditions and will take on different values depending on the considered time interval. In addition, the calculation of the RES installed capacity utilization factor with the above expression implies that the amount of electricity produced is known. That is, expression (1) can only be used for power plants already in operation.

Thus, determining the installed capacity utilization factor of generating power plants operating on the basis of RES requires forecasting. Several main approaches are used to forecast RES generation:

- application of autoregressive models for forecasting over very short planning horizons (an hour or less ahead) [9–14];
- use of probability distributions to determine the parameters of solar radiation and wind speed, followed by taking into account the efficiency of installations, the slope of solar panels and the orientation of wind turbines [15–19];
- application of forecasting models based on machine learning algorithms for direct generation forecast [20–26].

The probability distributions used to determine RES generation contain shape and scale parameters, the correct selection of which determines the forecast accuracy:

$$p(v) = \frac{k}{c}\left(\frac{v-u}{c}\right)^{k-1} \exp\left[-\left(\frac{v-u}{c}\right)^{k}\right], \quad (2)$$

where v is wind speed, m/s; k is the Weibull distribution form parameter; c is the Weibull distribution scale parameter, m/s; and u is the Weibull distribution terrain parameter, m/s.

$$f(E) = \frac{\Gamma(\lambda+\mu)}{\Gamma(\lambda)\Gamma(\mu)}\left(\frac{E}{E_m}\right)^{\lambda-1}\left(1-\frac{E}{E_m}\right)^{\mu-1}, \quad (3)$$

where E_m is the maximum value of solar radiation, kW/m^2; λ and μ are form parameters of the beta distribution; Γ is the gamma function.

These parameters vary depending on the geographical location of the territory under consideration, are empirical, and are contained in statistical reference books [27].

Today, the most convenient tools for forecasting renewable energy generation are forecasting models using machine learning algorithms. However, training such models requires large amounts of previously labeled data. Such data should contain the values of the features used for forecasting and the values of the target value for which a forecast is to be made. Therefore, after training, the model can take the values of the forecasting features and return the forecasting value of the target.

Modern metaheuristic methods are used in many fields to solve optimization tasks with multimodal and difficult-to-derive target functions [28–30]. In the power industry, these methods are applied to such problems as the optimization of the operating states of electrical motors [31], power loss reduction [32], configuration optimization of hybrid RES power plants [33], forecasting and equipment parameters estimation [34,35].

These approaches combine metaheuristics (such as dragonfly, grey wolves, best–worst, and group decision-making algorithms) to achieve better results and stability. Also, in these approaches, metaheuristics are used for tuning hyperparameters of machine learning forecasting models, in particular for wind speed forecasting.

Metaheuristic methods, rather than classical ones, provide good results in difficult cases, but the found solution could be nonstable.

The main idea of this research is to provide an approach for the forecasting and optimization of RES by combining metaheuristic methods with machine learning algorithms to achieve a high performance and stable results while using open-source data.

As far as the proposed approach assumes the use of open-source data, the process of data collection and its preparation is time-consuming. In that case, to achieve an adequate operation time, forecasting and optimization algorithms should provide the least possible number of series calculations. A small number of agents in the optimization algorithm allows the saving of time for computing but retains great performance in results. That outcome makes the proposed approach applicable in practical terms to real energy optimization problems.

This paper's structure is organized into the following sections: Section 2 contains the problem statement and defines the methods used for forecasting RES *CF* and placement optimization, followed by a mathematical formulation; the obtained results of the proposed forecasting and optimization algorithms are illustrated in Section 3; discussion of the results

and applicability of the proposed algorithm, as far as future plans placed for research, are placed in Section 4.

2. Materials and Methods

2.1. Capacity Factor Forecasting

In order to solve the problem of forecasting the RES installed capacity utilization factor, this study proposes forecasting models based on a random forest regressor. The models were trained on data concerning the operation of RES located in CIS countries, supplemented with average climate parameters over five years from the NASA database.

Given in Table 1 are fragments of the initial data for training models for predicting the installed capacity utilization factor for PVs and WPPs. In order to preserve the confidentiality of the geographic location of strategic energy infrastructure facilities, the values in the Latitude and Longitude columns are not given in this work.

Table 1. Fragment of wind and solar power plants' *CF* forecasting model training data.

Wind Power Plants							
$\mathbf{P_{inst}}$	**Latitude**	**Longitude**	$\mathbf{RH_{2M}}$	$\mathbf{T_{2M}}$	$\mathbf{WS_{10M}}$	$\mathbf{WS_{50M}}$	***CF***
3.49	xxxx	xxxx	88.147	5.822	2.452	4.618	0.357
3.30	xxxx	xxxx	83.383	7.603	4.540	6.538	0.353
2.50	xxxx	xxxx	88.147	5.822	2.452	4.618	0.356
1.75	xxxx	xxxx	83.383	7.603	4.540	6.538	0.353
35	xxxx	xxxx	82.207	4.593	4.970	6.705	0.281
1.65	xxxx	xxxx	84.822	2.848	4.740	6.703	0.068
25.20	xxxx	xxxx	82.207	4.593	4.970	6.705	0.290
25.20	xxxx	xxxx	82.207	4.593	4.970	6.705	0.316
49.40	xxxx	xxxx	70.970	9.735	4.532	6.440	0.318
Solar Power Plants							
$\mathbf{P_{inst}}$	**Latitude**	**Longitude**	$\mathbf{SW_{DIFF}}$	$\mathbf{SW_{DNI}}$	$\mathbf{SW_{DWN}}$	$\mathbf{SR_{FALB}}$	$\mathbf{RH_{2M}}$	$\mathbf{T_{2M}}$	***CF***
0.50	xxxx	xxxx	1.498	3.157	3.107	0.198	82.948	7.027	0.164
0.87	xxxx	xxxx	1.498	3.157	3.107	0.198	82.948	7.027	0.165
0.63	xxxx	xxxx	1.498	3.157	3.107	0.198	82.948	7.027	0.164
2	xxxx	xxxx	1.498	3.157	3.107	0.198	85.228	6.347	0.164
25	xxxx	xxxx	1.500	3.668	3.325	0.218	79.032	5.080	0.149
15	xxxx	xxxx	1.573	4.115	3.707	0.263	69.752	7.543	0.151
10	xxxx	xxxx	1.573	4.115	3.707	0.263	71.468	7.000	0.153
45	xxxx	xxxx	1.592	3.743	3.465	0.273	75.365	4.917	0.132

The data for training the forecasting model includes the following parameters:

- P_{inst} is the installed capacity of the RES generation power facility, MW;
- SWDIFF is the diffuse (light energy scattered out of the direction of the sun) solar irradiance incident on a horizontal plane at the surface of the Earth under all sky conditions, kW/m^2;
- SWDNI is the direct solar radiation incident on a horizontal plane on the Earth's surface, kW/m^2;
- SWDWN is the total solar radiation incident on a horizontal plane on the Earth's surface, kW/m^2;
- RH2M is the ratio of the actual partial pressure of water vapor to the partial pressure at saturation at a height of 2 m (relative humidity), %;
- T2M is the average air temperature at a height of 2 m above the ground, °C;
- SRFALB is the ratio of solar energy reflected by the Earth's surface to the total solar energy incident on the Earth's surface, p.u.;
- WS10M, WS50M is the average annual wind speed at a height of 10 and 50 m above the ground, respectively, m/s;

- Latitude is the value of geographic latitude characterizing the location of the power facility, deg;
- Longitude is the value of geographic longitude characterizing the location of the power facility, deg;
- *CF* is the installed capacity utilization factor of the power facility, p.u.

The dimensions of the initial data used to train forecasting models were 94 rows and 11 columns for WPPs and 141 rows, 7 columns for PVs. The data were divided into training and test sets in a 70/30 ratio. For forecasting the *CF*, the forecasting model parameters presented in Table 2 were used.

Table 2. Forecast models hyperparameters.

Wind Power Plants		
Model	**Number of Estimators**	**Maximum Features**
Random forest	61	3
Solar Power Plants		
Model	**Number of Estimators**	**Maximum Features**
Random forest	141	4

The complexity of forecasting the RES *CF* is expressed, among other things, in the absence of a strong dependence on the features used, which is a consequence of the stochastic nature of the predicted parameter. The significance of the features for the models used in forecasting the RES *CF* is shown in Figure 1. In the case of forecasting the PV's *CF*, the relationship with average annual climatic parameters is stronger than in the case of forecasting the WPP's *CF*. However, the dependence of the RES *CF* on the facility's geographical location and its installed capacity is predominant.

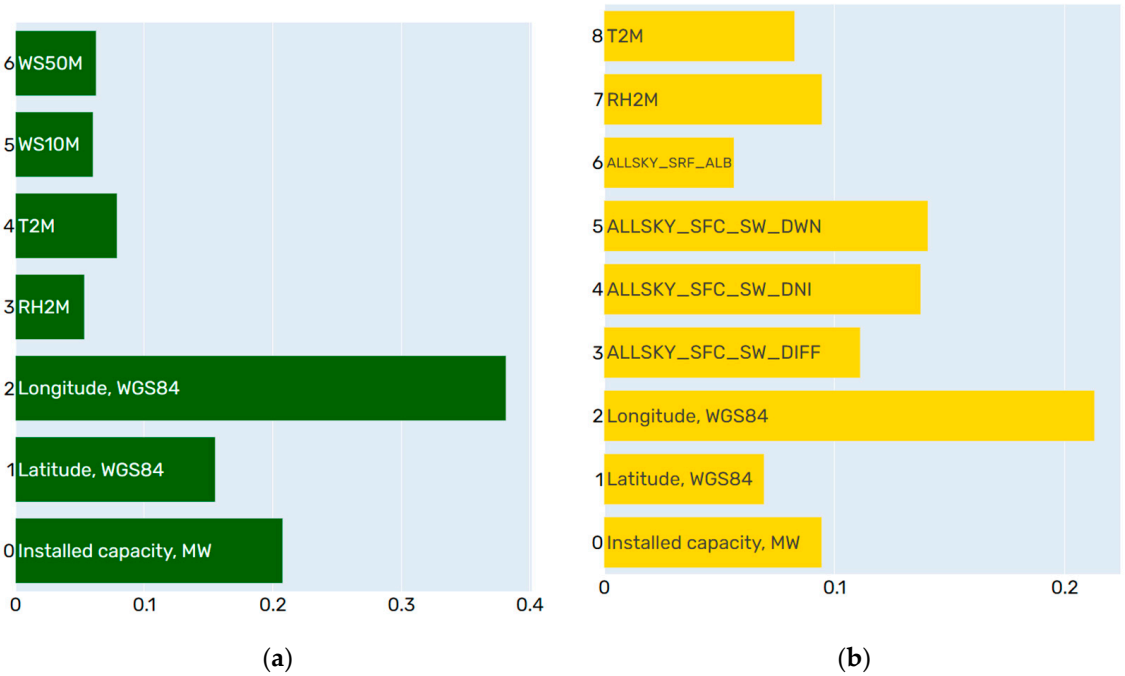

(**a**) (**b**)

Figure 1. Model feature importance: (**a**) for the forecasting model of the wind power plant capacity factor; (**b**) for the forecasting model of the PV power plant capacity factor.

2.2. RES Placement Optimization

Within the framework of this study, part of optimization is to find options for the optimal geographical location of RES in order to maximize the capacity factor. The objective function within the task's framework is the *CF* of a power plant. The *CF* is determined using the forecasting models described in the first part of this study.

In general, the optimization problem can be represented as follows:

$$CF = f(X, Y) \rightarrow \max_{g}, \tag{4}$$

where X, Y are vectors of independent and dependent variables and g is restrictions.

Geographical coordinates (longitude and latitude), which determine the position of a power facility, are independent variables. The dependent variables include all the annual mean meteorological parameters used by the model to calculate the *CF* value.

The location of the power plant within the boundaries of the selected area (region, territory, republic, etc.) is used as a constraint for the problem being solved:

$$g : p \in A, \tag{5}$$

where p is a point (the geographical location of the power plant) and A is the allowable area (the area within the boundaries of the selected territory).

The form of the objective function (the dependence of *CF* on geographical coordinates) for WPPs and PVs is shown in Figures 2 and 3. The forecasting model is used to calculate the values of the target function (capacity 3D representation of the *CF* forecast using a random forest algorithm, where axis X and Y correspond to the geographical location of the area and the Z axis represents target function value).

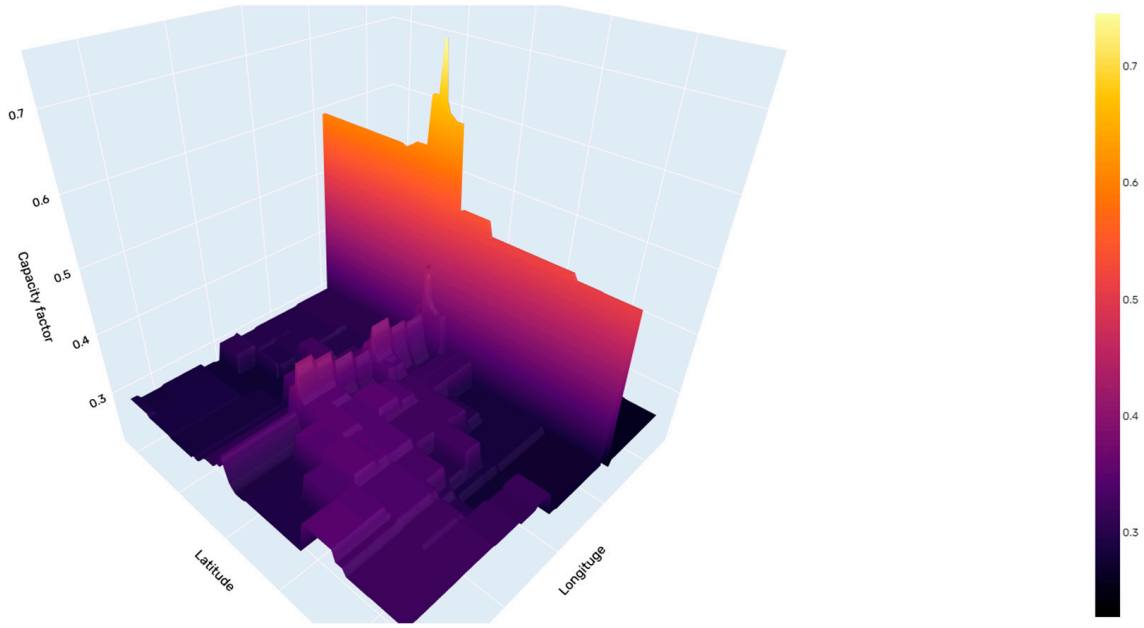

Figure 2. 3D visualization of target function for a 15 MW wind power plant.

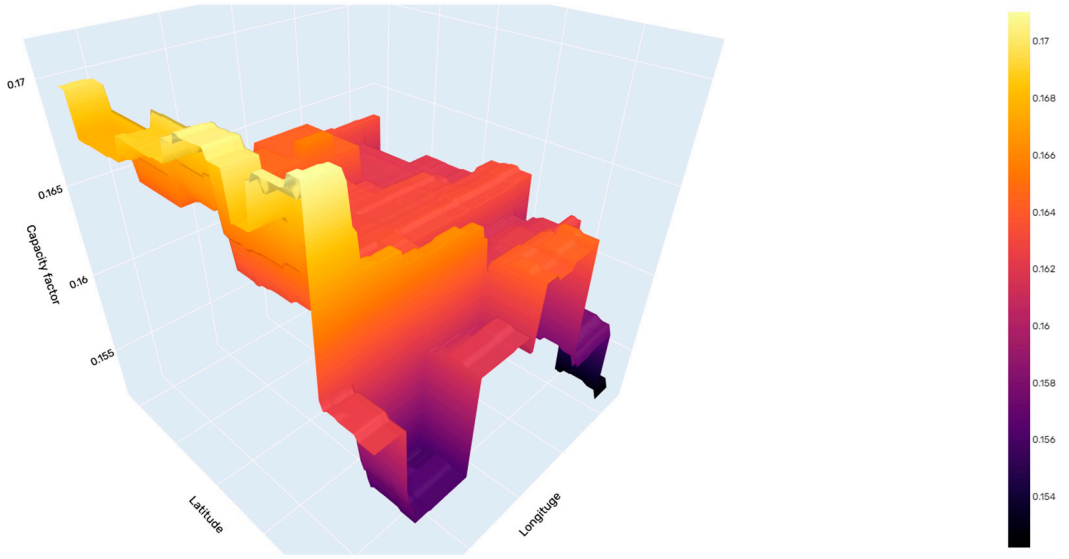

Figure 3. 3D-visualization of the target function for a 15 MV PV power plant.

For optimization, it is advisable to use heuristic algorithms based on the principles of swarm intelligence, since the form of the objective function is multi-extremal and does not have an analytical form.

The values of the dependent variables are determined with the NASA POWER API [36]. Upon request and specifying the geographical coordinates of a point, a data array containing a number of parameters is returned. This array is processed; as a result, the average annual parameters can be obtained. The duration of the processing of one API request depends on the number of parameters returned and the time interval. Within the framework of this study, the processing time for requests for a WPP was about seven seconds and about 15 s for a PV.

The lengthy process of obtaining the meteorological parameters necessary for optimization imposes limitations on the calculation time of the optimization algorithms used. Thus, an algorithm is required that does not require a large number of agents, has a fast convergence, and has a function for controlling the degree of stochasticity of agents.

Such an algorithm is the grey wolf optimizer (GWO), widely used to solve optimization problems [37–41]. The algorithm is based on a mathematical model of the behavior of grey wolves during hunting. There is a strict hierarchy according to which all wolves in a pack can be classified:

- at the first step of the hierarchy is the alpha wolf;
- the beta wolf is located on the second step of the hierarchy;
- the third most important in the pack is the delta wolf;
- the remaining individuals are equal and are called omega wolves.

During the hunt, the leader is the alpha wolf. In addition, beta and delta individuals are auxiliary landmarks. Wolves are positioned in such a way as to surround the prey. At the same time, the expected prey position of omega wolves is determined based on the location of the leading individuals (alpha, beta and delta). The mathematical model describing the hunting of the pack is as follows:

$$\begin{array}{c} \overline{D} = \left|\overline{C} \cdot \overline{X_p}(t) - \overline{X}(t)\right| \\ \overline{X}(t+1) = \overline{X_p}(t) - \overline{A} \cdot \overline{D} \end{array}, \quad (6)$$

where $\overline{X}$ is a vector describing the position of the agent (wolf); $\overline{X_p}$ is a vector describing the position of the supposed optimum (prey); A, C are vectors of calculated coefficients; and t is the current calculation iteration.

At each iteration, the position of all agents is updated according to the position of the alpha, beta, and delta individuals:

$$\begin{array}{c} \overline{D_i} = \left|\overline{C} \cdot \overline{X_i}(t) - \overline{X}(t)\right|, \; i \in \{\alpha, \beta, \delta\} \\ \overline{X_1}(t) = \overline{X_\alpha}(t) - \overline{A_1} \cdot \overline{D_\alpha} \\ \overline{X_2}(t) = \overline{X_\beta}(t) - \overline{A_2} \cdot \overline{D_\beta} \\ \overline{X_3}(t) = \overline{X_\delta}(t) - \overline{A_3} \cdot \overline{D_\delta} \end{array}, \tag{7}$$

where $\overline{D_i}$ is the correction vector and $\overline{X_1}$, $\overline{X_2}$, $\overline{X_3}$ are vectors with the updated positions of all agents, according to the three best agents (α, β, γ).

$$\overline{X}(t+1) = \frac{\overline{X_1} + \overline{X_2} + \overline{X_3}}{3}. \tag{8}$$

where $\overline{X}$ is the resulting vector with the updated positions of all agents.

Coefficients A and C are determined as follows:

$$\begin{array}{c} \overline{A} = 2 \cdot a \cdot \overline{r_1} \\ \overline{C} = 2 \cdot \overline{r_2} \end{array}, \tag{9}$$

where a is a coefficient decreasing linearly in the interval [2, 0] according to the number of the current iteration, and r_1, r_2 are random values in the interval [0, 1].

The required number of agents for this algorithm is comparable to the size of a pack of grey wolves and ranges from 7 to 15. The small number of agents of the algorithm determines its applicability within the framework of this problem (the time of one iteration of the calculation is 1.75–3.75 min with the maximum number of agents).

A graphical interpretation of the principle of changing the position of agents is shown in Figure 4.

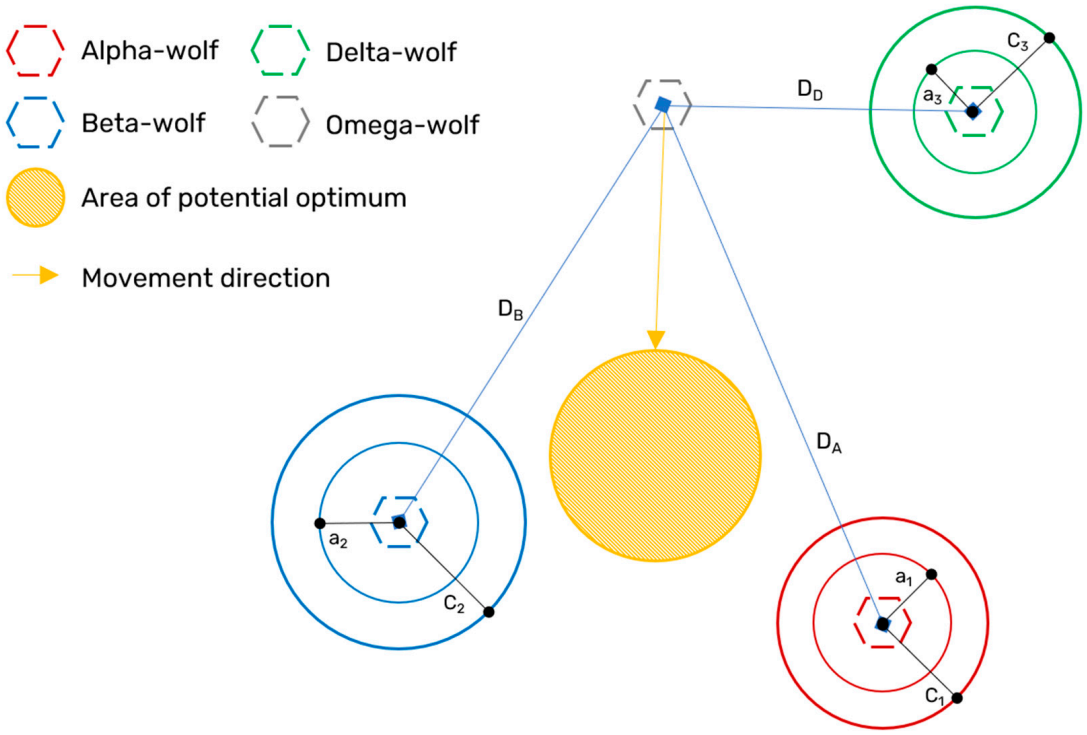

Figure 4. Visualization of agent movement during optimization.

In the classical GWO algorithm, the coefficients determine the movements of agents (wolves), while changing parameter a from 2 to 0 changes the optimization stage. In the interval when a is greater than 1, the system is in the search stage (agents are dispersed in order to cover the widest search area possible). When parameter a is less than 1, then the system goes into the hunting stage (all agents move towards the optimum found at the previous stage).

This approach works correctly when optimizing functions that depend on abstract numerical parameters. However, when calculating coefficients A and C according to expressions (9), within one iteration of the calculation, the agents' coordinates increment too much (a change in latitude or longitude by 1 degree corresponds to a change in the agents' position by approximately 110 km). This leads to their ejection outside the established optimization boundaries. In order to exclude the release of agents beyond the established boundaries, additional coefficients equal to 0.2 and 1.5, respectively, were selected to calculate the vectors of coefficients A and C.

The flow chart of the proposed algorithm is shown in Figure 5.

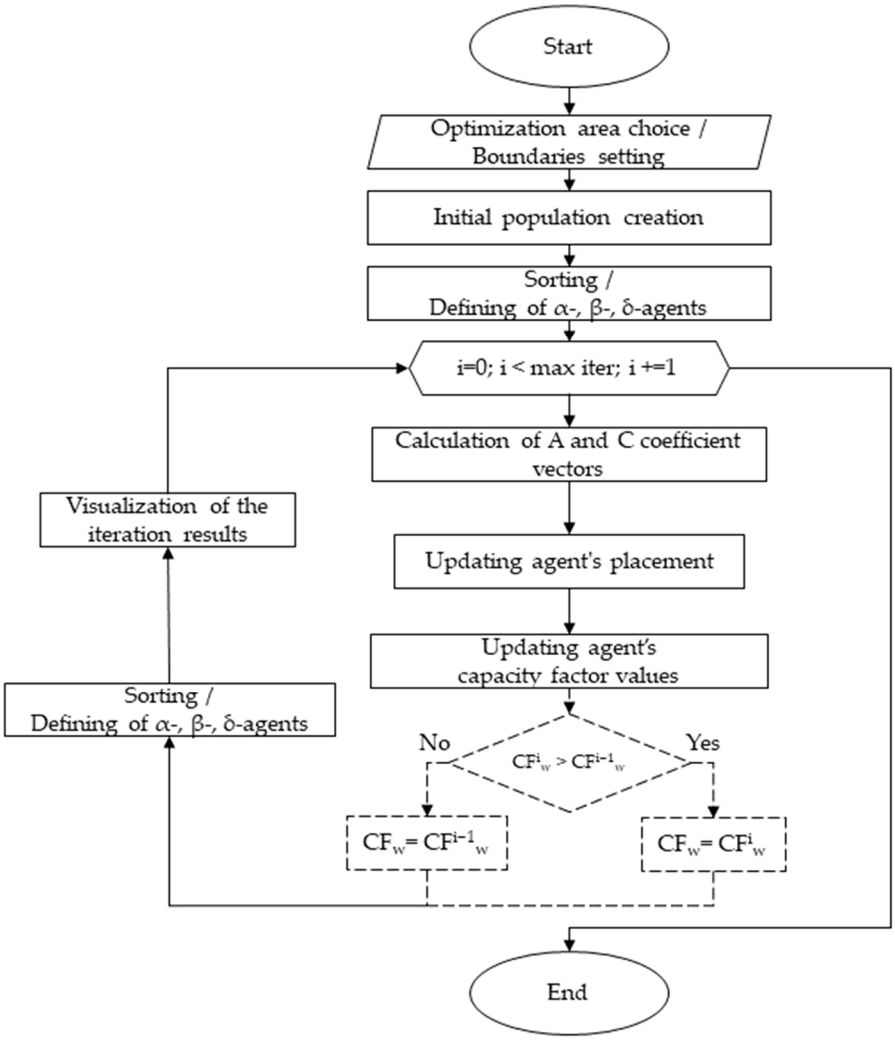

Figure 5. Optimization algorithm flowchart.

The positions of agents in the initial population are determined by a random choice of coordinates from a 10,000 × 10,000 grid obtained from a given optimization area. In the initial population, the roles of alpha, beta, and delta individuals are distributed depending on the *CF* value. The same thing happens at the end of each iteration.

The criterion for stopping the algorithm is the completion of a given number of iterations. This criterion is a standard stopping criterion for heuristic algorithms when optimizing a complex multi-extremal function. The criterion of the minimum increment of the objective function in this case is not used as a stopping criterion, since during the optimization process, agents may temporarily "get stuck" at the point of local optimum. However, after several iterations of the calculation, the next best solution, which can be prevented by stopping the algorithm according to the criterion of the minimum increment of the objective function, can be found.

The forecasting model is used to calculate the values of the target function (the capacity factor) for each agent during the optimization process. The location (latitude and longitude) of the agent, together with the meteorological parameters, are used as the features for the forecasting model, and the result of the forecasting model is the value of the target function for the considered agent. When agents' positions are updating, the target function values recalculate again according to the process described above.

The block for checking the increase in the *CF* of agents, represented by a dashed line in Figure 6, allows for the creation of a "greedy" algorithm in which the position of agents changes only when the objective function changes towards the optimum.

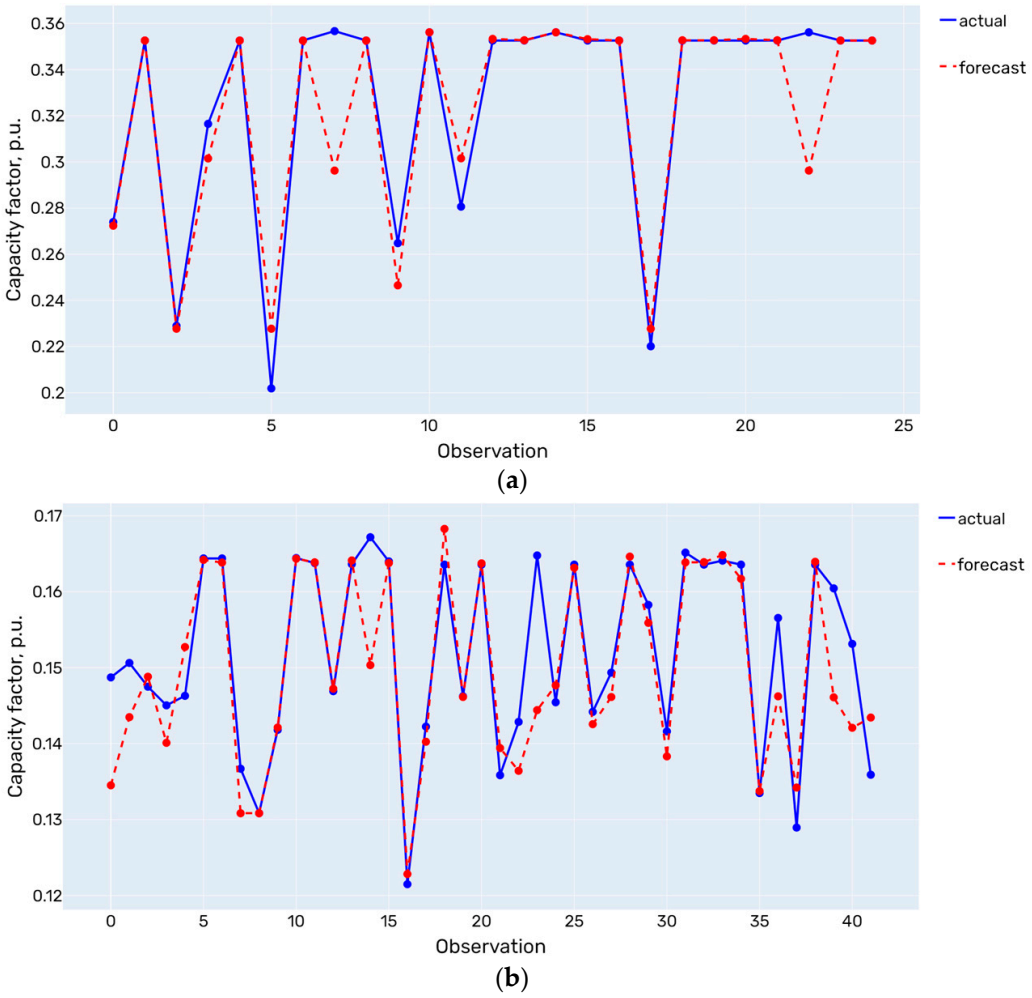

Figure 6. Forecasting model performance on test data: (**a**) for predicting the wind power plant capacity factor; (**b**) for predicting the solar power plant capacity factor.

3. Results

3.1. Capacity Factor Forecasting

When validating the models with the cross-validation method, the training sample was randomly divided into five parts. The metrics expressing the quality of the model forecast [42,43] for the validation and testing stages are presented in Tables 3 and 4. The predicted value (*CF*) has a range of change from 0 to 1 p.u. (or from 0 to 100 as a percentage). Therefore, metrics representing the model score in named units (MAE, MSE, etc.) were not used. Instead, metrics that express the model results as percentages (nMAE, explained variance) are provided. In addition, to evaluate the largest deviation of the forecast from the actual values, the values of the maximum error (Max_error) are given. A graphical representation of the results of predictive models on a test sample is shown in Figure 6.

Table 3. Evaluation metrics of the capacity factor forecasting model for wind power plants.

Cross-Validation Results			
RMSE, p.u.	**Max_Error, p.u.**	**nMAE, %**	**Explained Variance, %**
0.1302	0.2082	52.8	86.6
0.0519	0.1242	24.9	97.9
0.0633	0.1555	32.5	95.4
0.0229	0.0502	5.2	81.4
0.0523	0.1348	11.7	96.9
Test Data Results			
RMSE, p.u.	**Max_Error, p.u.**	**nMAE, %**	**Explained Variance, %**
0.0189	0.06	2.8	85.3

Table 4. Evaluation of the capacity factor forecasting model for PV power plants.

Cross-Validation Results			
RMSE, p.u.	**Max_Error, p.u.**	**nMAE, %**	**Explained Variance, %**
0.0071	0.015	3.6	72.5
0.0091	0.0202	3.9	57.4
0.0098	0.0191	5.1	42.8
0.0206	0.0611	11.3	30.7
0.0071	0.0167	2.9	75.2
Test Data Results			
RMSE, p.u.	**Max_Error, p.u.**	**nMAE, %**	**Explained Variance, %**
0.006	0.0204	2.5	76.4

The average absolute normalized error (nMAE) is 23.7% for the forecast model of the *CF* of WPP and 5.13% for the forecast model of the *CF* of PV. The average level of the explained variance of stochastic processes is 90.75% and 60.1%, respectively, for WPPs and PVs. Based on the above metrics and graphical representation of the data, it can be concluded that the resulting models make a stable forecast with high accuracy. Thus, despite the use of open data and a small amount of initial data, such models can be used as part of solving the problem of optimizing the placement of RES power plants to calculate the values of the *CF* as the objective function.

3.2. RES Placement Optimization

In order to determine the influence of the agent *CF* comparison block on the algorithm results, the results of two versions of the algorithm were compared, greedy GWO and basic GWO. Table 5 shows the optimization results for two versions of the algorithm. The "Inside" indicator shows whether the found solution is within the established boundaries of the problem or not.

During optimization with the basic GWO algorithm, the final solution is often outside the considered boundaries; during optimization, the value of the objective function decreases (instead of the expected increase). As a result, it can be concluded that it does not make sense to use the basic GWO algorithm for this problem. On the contrary, the modified greedy GWO algorithm stably returns solutions that are within the established boundaries and allows for determining several local optima. On average, the *CF* maximization for the placement of power plants based on RES for the greedy GWO algorithm is 0.166 percentage points for wind farms.

Table 5. Comparison of two algorithm modifications for wind power plant optimization.

Run	Greedy GWO				Basic GWO			
	Initial Best	**Final Best**	**Difference**	**Inside**	**Initial Best**	**Final Best**	**Difference**	**Inside**
1	0.3497	0.4091	0.0594	Yes	0.5977	0.3374	−0.2603	Yes
2	0.5179	0.7219	0.2040	Yes	0.3463	0.3443	−0.0020	No
3	0.3491	0.4091	0.0600	Yes	0.3723	0.3186	−0.0537	No
4	0.3533	0.3971	0.0437	Yes	0.3448	0.3205	−0.0243	No
5	0.3488	0.7449	0.3961	Yes	0.3502	0.3492	−0.0010	Yes
6	0.5978	0.7449	0.1471	Yes	0.3971	0.3450	−0.0521	Yes
7	0.5180	0.7449	0.2269	Yes	0.5179	0.3389	−0.1790	Yes
8	0.6756	0.6756	0	Yes	0.3502	0.6572	0.3070	Yes
9	0.6067	0.7219	0.1151	Yes	0.5979	0.3504	−0.2475	Yes
10	0.3412	0.7449	0.4037	Yes	0.3750	0.3176	−0.0574	No
Average maximization			**0.1656**		**Average maximization**		**−0.0570**	

A comparison of the optimums found by the algorithm with a two-dimensional display of the objective function for WPPs and PVs is shown in Figures 7 and 8. Figures 7 and 8 show the location of the agents during the last iteration of the proposed algorithm with green or blue polygons, and the background of the map is the contour representation of the 3D target function shown in Figures 2 and 3.

A detailed illustration of all iterations of one algorithm calculation for a 15 MW wind farm is presented in Appendix A.

The comparison of the proposed GWO to other commonly used metaheuristic algorithms such as firefly optimization algorithm (FFO), particle swarm optimization algorithm (PSO) and basic random search is presented in Figure 9 and in Table 6. The convergence curves for considered algorithms are shown in Figure 10.

Table 6. Statistical metrics for evaluation of optimization results for wind power plant optimization achieved using various algorithms.

	Algorithm			
Metric	**Random Search**	**PSO**	**FFO**	**GWO**
Mean	0.207699	0.466938	0.459489	0.480645
Median	0.205152	0.493582	0.409117	0.397110
Standard deviation	0.009906	0.009906	0.137109	0.146610
Maximal	0.146610	0.527894	0.527894	0.744965
Minimal	0.195894	0.195894	0.195894	0.324952
Mean deviation from global maximum	−0.532301	−0.273062	−0.280511	−0.259355
Median deviation from global maximum	−0.534848	−0.246418	−0.330883	−0.342890

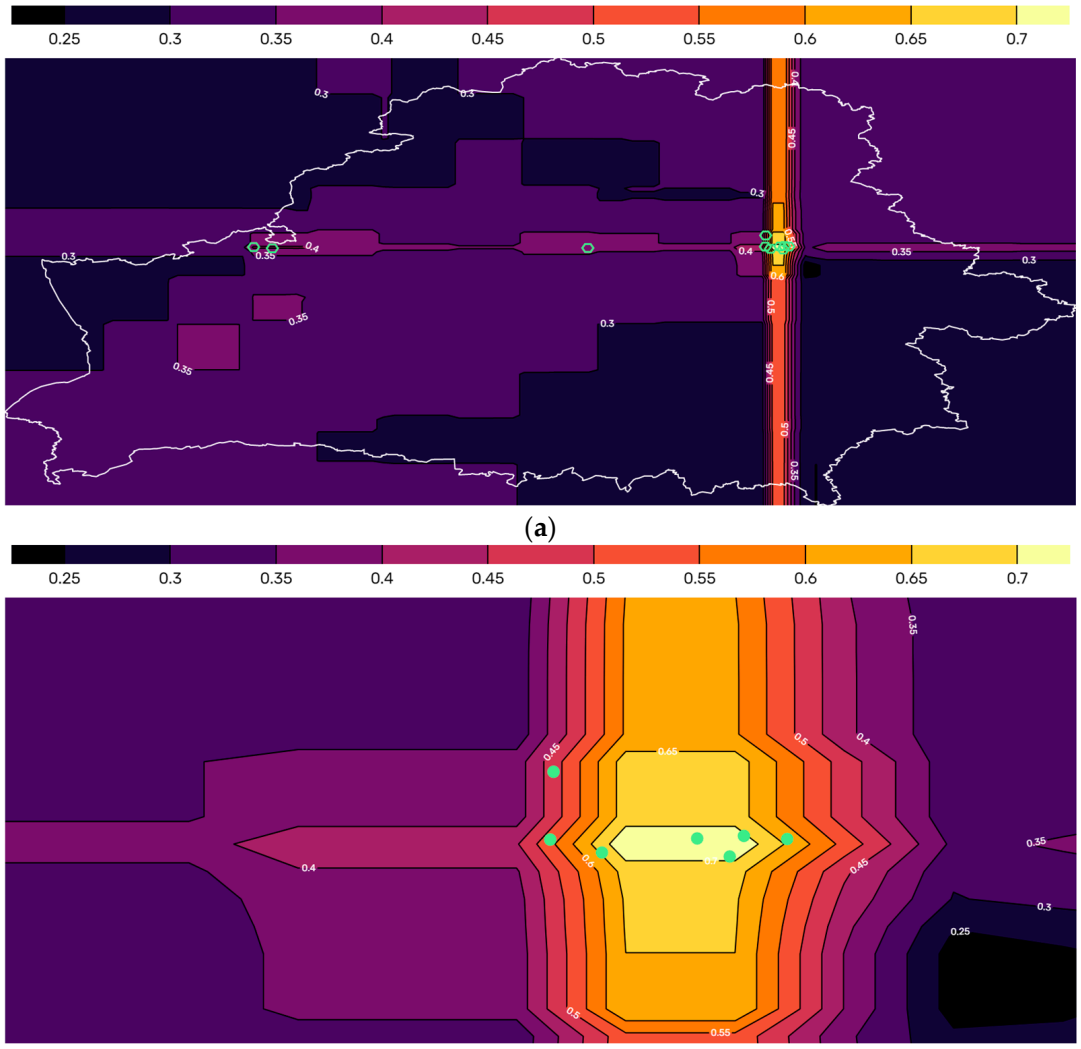

Figure 7. Results of 10 runs for a 15 MW wind power plant placement optimization: (**a**) whole area; (**b**) zoomed-in to global optima.

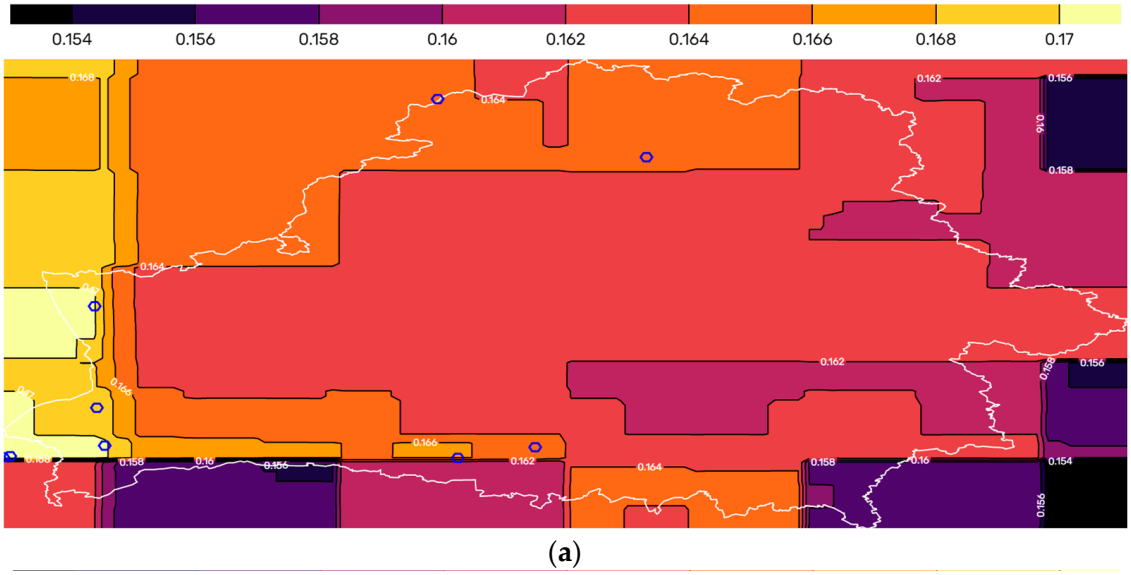

Figure 8. *Cont.*

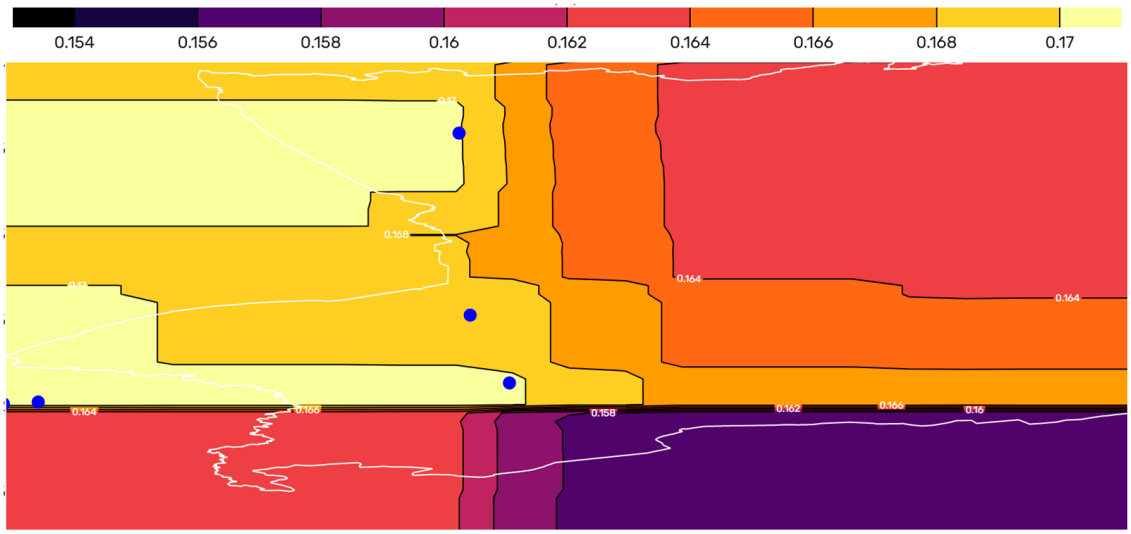

(**b**)

Figure 8. Results of 10 runs for a 15 MW PV power plant placement optimization: (**a**) whole area; (**b**) zoomed-in to global optima.

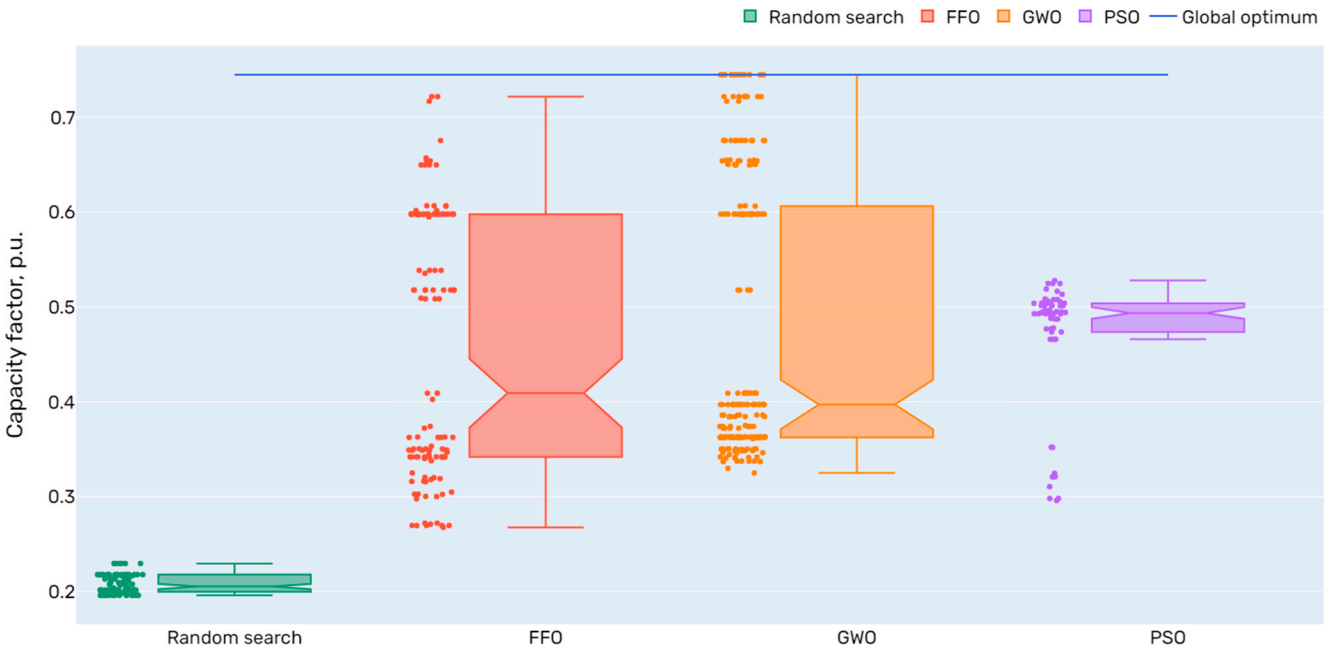

Figure 9. Boxplot visualization of optimization results for wind power plant optimization achieved using various algorithms.

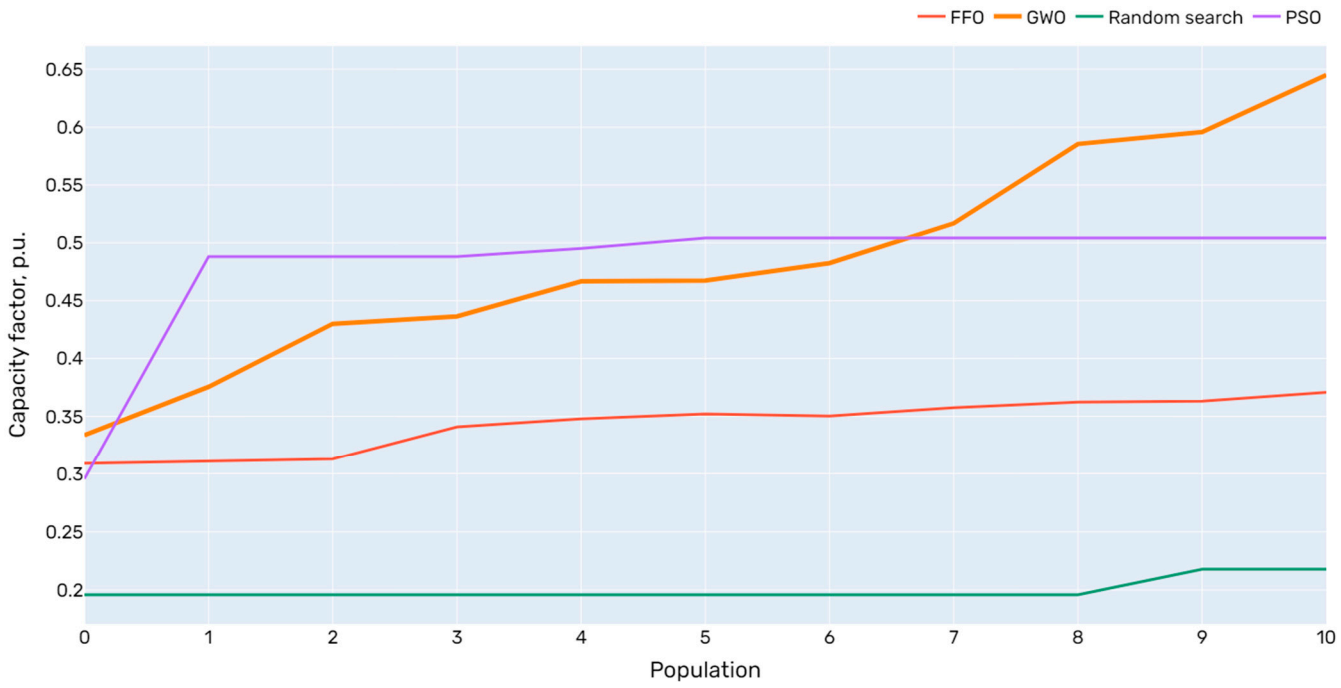

Figure 10. Example of convergence curves of optimization results for wind power plant optimization achieved using various algorithms.

4. Discussion

In this study, a system for the collection and processing of the meteorological data necessary for forecasting the RES *CF* was created. Regression models based on machine learning algorithms were also proposed to forecast the *CF* of RES. The proposed models were trained on open data on the operation of energy facilities and meteorological data. As a result, the models showed high accuracy in predicting the stochastic variable, explaining about 90% of the variance in the distribution of WPP *CF* and about 60% of the variance of PV *CF*.

The forecasting results for the RES *CF* were integrated into the modified GWO optimization algorithm as an objective function. The basic GWO algorithm has been modified and tuned to solve the problem of optimizing the placement of RES-based power plants in order to maximize their *CF*.

Basic GWO is not applicable for optimizing the placement of RES-based power plants in order to maximize their *CF*. This is due to overly large increments of agent coordinates, which leads to the release of the final solution outside the considered area. To use GWO to solve this type of problem, it is necessary to adjust additional coefficients for vectors and save the final solution within the considered area. The use of greedy GWO makes it possible to eliminate the loss of the area with a high *CF* identified during optimization.

Based on the results of greedy GWO presented, it can be concluded that the algorithm copes with the optimization problem by identifying areas with high *CF* values for both WPPs and PVs. The area of the optimal solution found by the algorithm for WPPs coincides with the area of the global optimum of the objective function in seven out of 10 cases, for PV in six out of 10. The remaining solutions (3/10 for WPPs and 4/10 for PVs) correspond to local optima.

It is worth noting that the hexagons depicted in Figures 7 and 8, as well as in Appendix A, represent an area of about 10 square kilometers (simulating the area covered by real power plants based on RES with a capacity of up to 30 MW), and the geometry of this area can be changed. Such a format for displaying the results makes it possible to evaluate the distribution of the *CF* over the power plant territory, taking into account its geometry.

During optimization, the algorithm not only determines the global optimum of the multi-extremal *CF* distribution function depending on geographical location but also suggests several potential areas for locating power plants with a high *CF*. The figures in Appendix A demonstrate the alignment of agents along the latitudinally extended region with the highest *CF* values (more than 0.5 p.u.).

Comparison of the proposed GWO against commonly used metaheuristics (FFO, PSO) and random search shows that the random search approach does not apply for such optimization problems because of the narrow areas of the high target function values. FFO and GWO perform far more greatly with similar mean results (0.4 and 0.39) and spread of found solutions. However, the proposed approach against the others has the potential to reach the global optimum and areas near the global optimum. PSO has great stability in the results on one side, but the other found solutions lie farther from the global optimum against the proposed algorithm. The results of the evaluation and comparison of the proposed algorithm show that it is competitive against modern state-of-the-art optimization approaches applied to the considered problem. Thus, this system, which consists of two algorithms for forecasting the *CF* and optimizing the placement of power plants based on RES and trained on open data, can be used for practical application to the real power industry problems regarding both assessment of the energy potential of territories and the planning of the placement of real power facilities, in addition to the evaluation of efficiency and power production for the realization of green certificates. However, this system still cannot be implemented in real-time decision support systems because of time-consuming data processing.

Regarding the theoretical and educational fields, the proposed approach could be used as a methodology in R&D projects related to energy optimization and as the base for further improvements.

Future work in this field will be aimed at the reduction of open-source data processing time, searching for new data sources, and modifications of proposed algorithms using further comparative analysis and hybridization with other optimization methods.

Author Contributions: Conceptualization, A.M.B., S.A.E. and A.I.K.; methodology, A.M.B. and P.V.M.; software, A.M.B., validation, A.M.B.; writing—original draft preparation, A.M.B., S.A.E. and A.I.K.; writing—review and editing, S.A.E.; visualization, A.M.B.; supervision, A.I.K. and P.V.M. All authors have read and agreed to the published version of the manuscript.

Funding: The research was carried out within the state assignment with the financial support of the Ministry of Science and Higher Education of the Russian Federation (subject No. FEUZ-2022-0030 Development of an intelligent multi-agent system for modeling deeply integrated technological systems in the power industry).

Institutional Review Board Statement: Not applicable.

Informed Consent Statement: Not applicable.

Data Availability Statement: Not applicable.

Conflicts of Interest: The authors declare no conflict of interest.

Appendix A

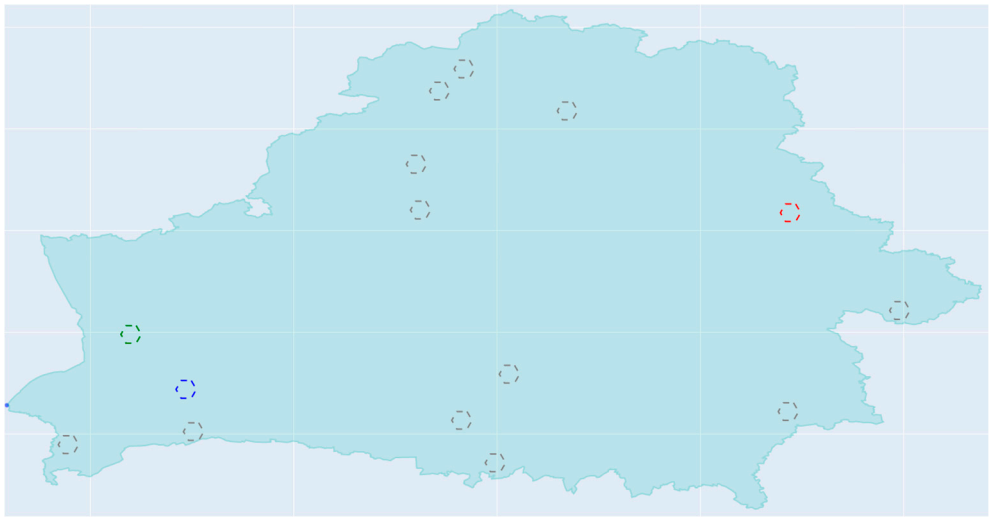

(**a**)

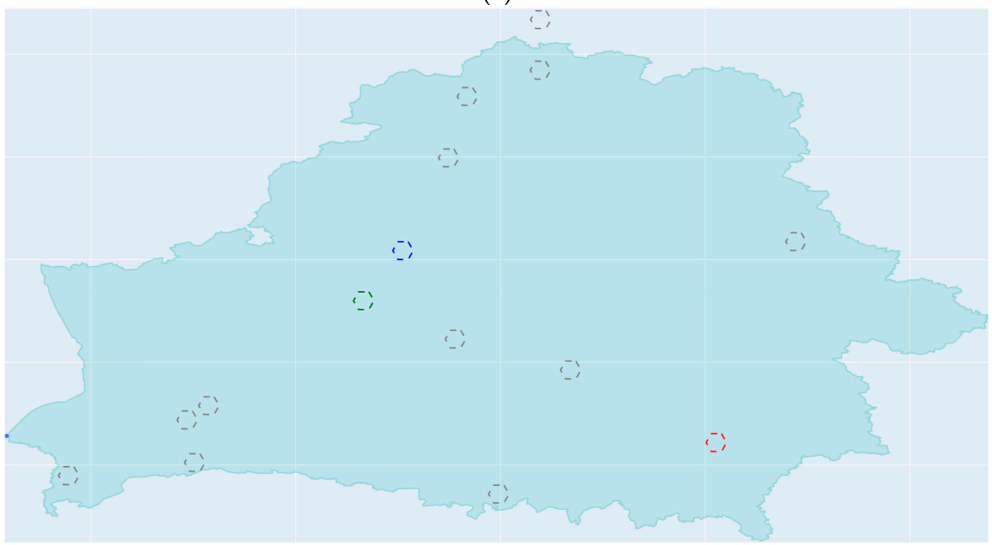

(**b**)

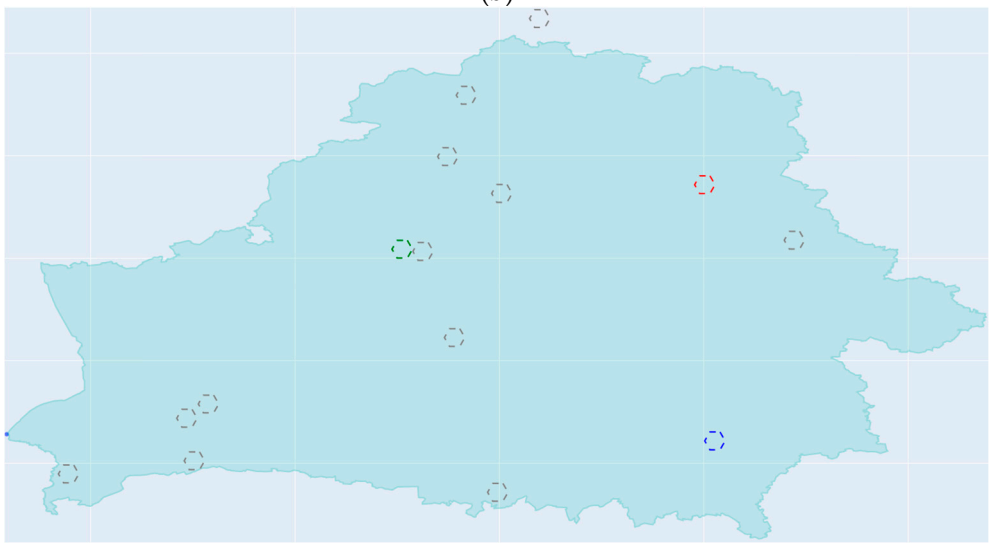

(**c**)

Figure A1. *Cont.*

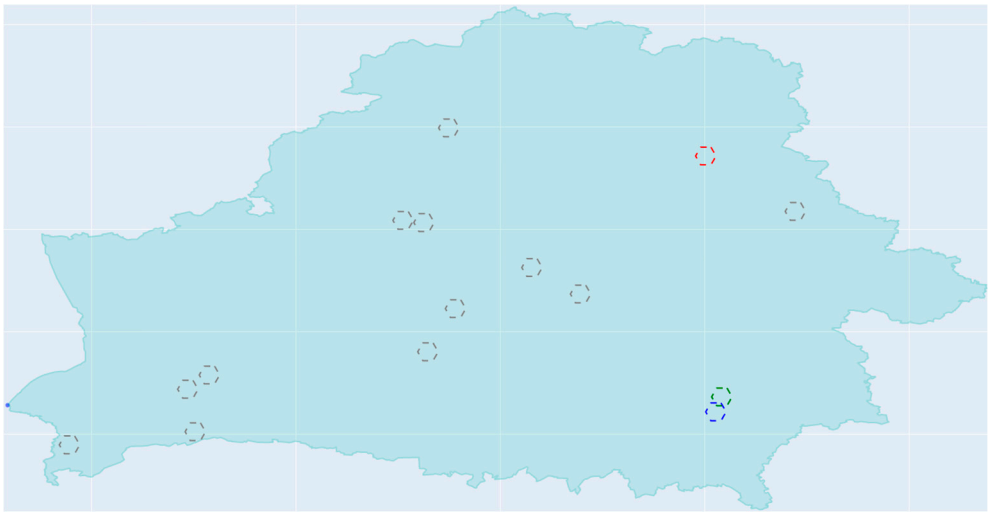

(**d**)

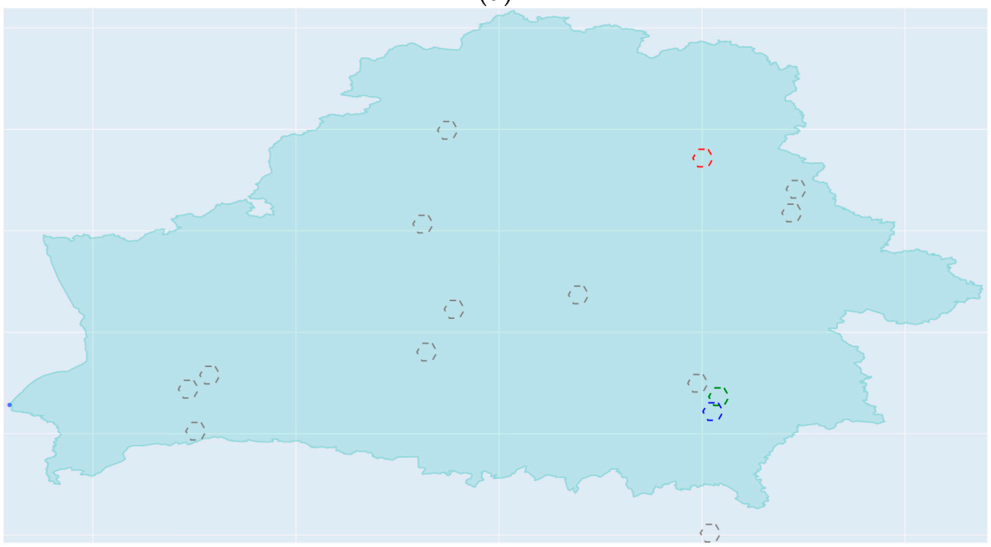

(**e**)

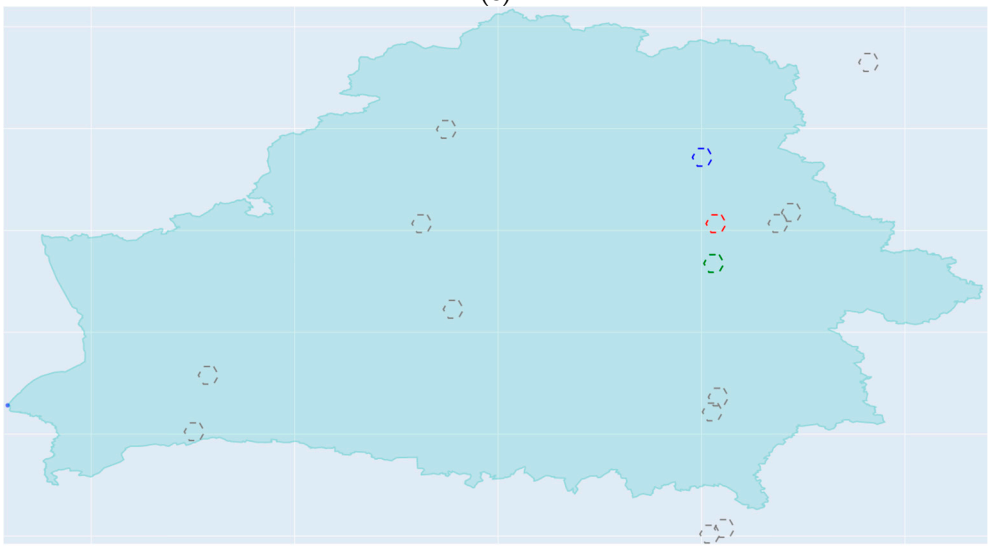

(**f**)

Figure A1. *Cont.*

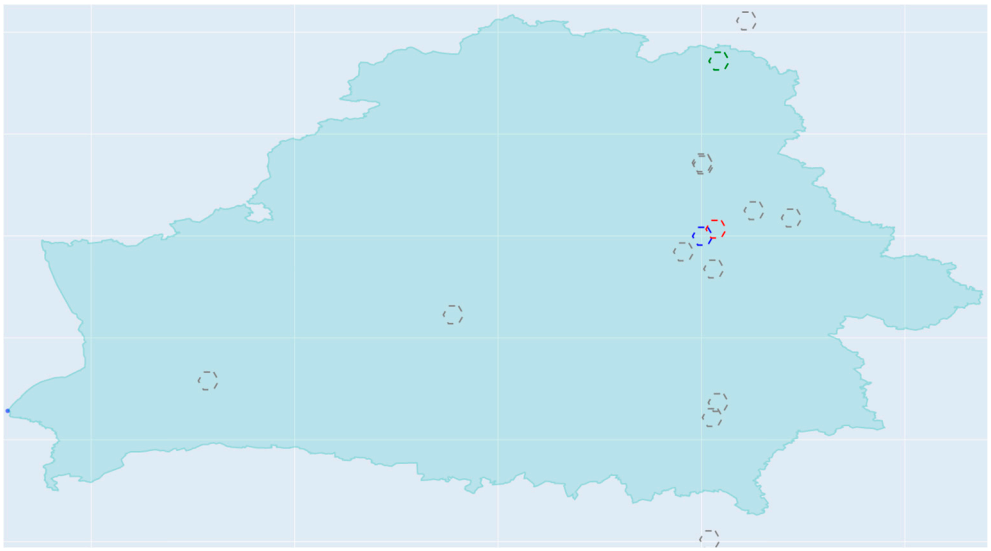

(**g**)

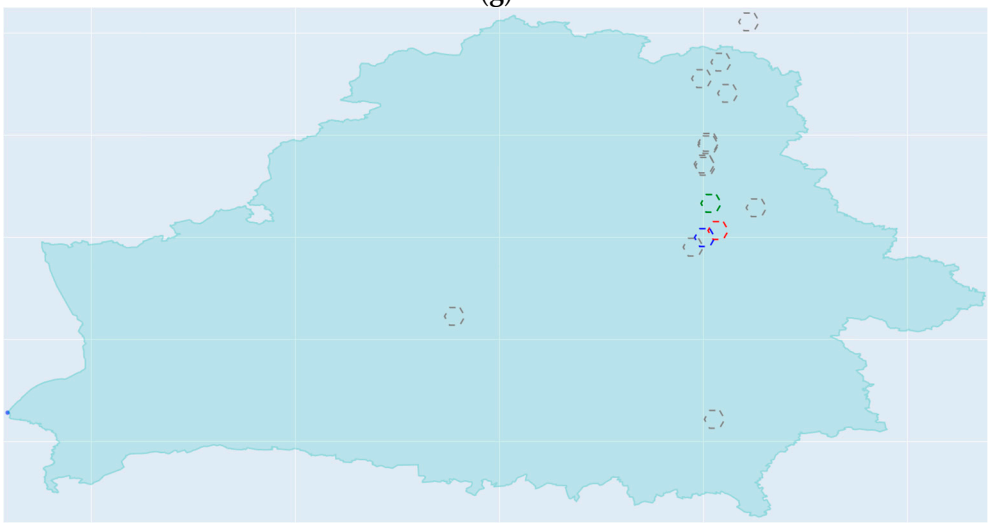

(**h**)

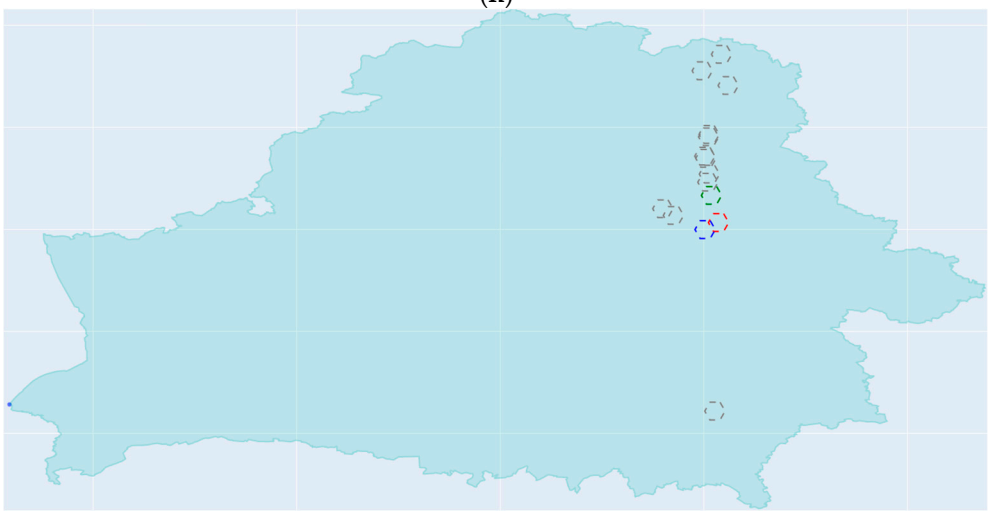

(**i**)

Figure A1. *Cont*.

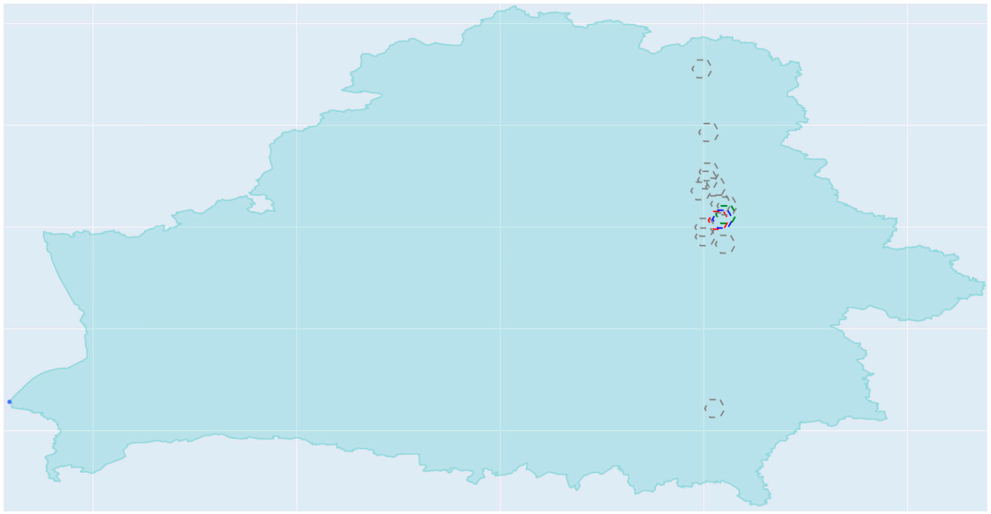

(**j**)

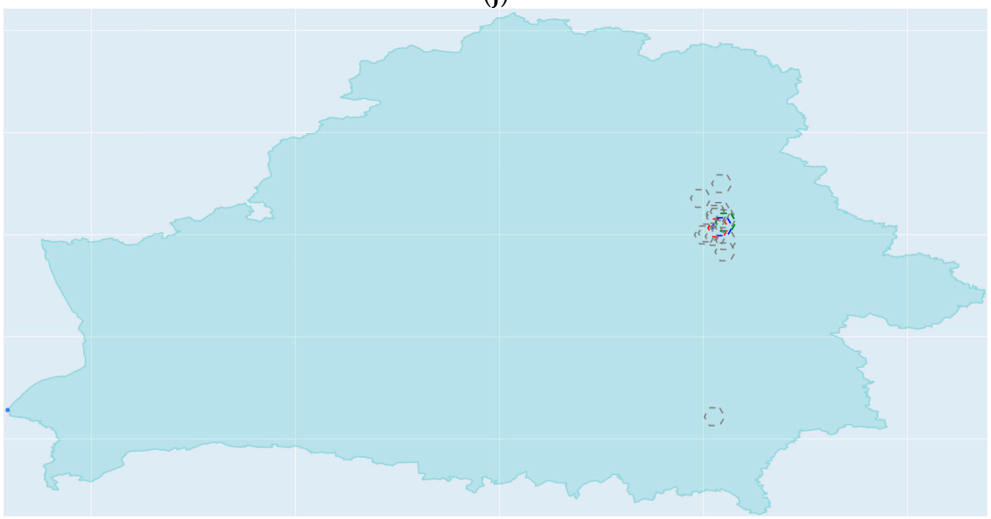

(**k**)

Figure A1. Visualization of the whole process for 15 MW wind power plant optimization: (**a**) is first population, (**b**–**k**) are first 10 iterations of the algorithm. Red, blue and green hexagons represent alpha, betta and delta wolves, grey ones represent omega wolves.

References

1. Upward Revisions to Renewable Capacity Expansion Forecasts from Renewables 2021 to Renewables 2022. Available online: https://www.iea.org/data-and-statistics/charts/upward-revisions-to-renewable-capacity-expansion-forecasts-from-renewables-2021-to-renewables-2022 (accessed on 5 February 2023).
2. Setting the Record Straight about Renewable Energy. Available online: https://www.wri.org/insights/setting-record-straight-about-renewable-energy (accessed on 19 February 2023).
3. How to Transform the Energy System and Reduce Carbon Emissions. Available online: https://www.irena.org/Digital-content/Digital-Story/2019/Apr/How-To-Transform-Energy-System-And-Reduce-Carbon-Emissions (accessed on 19 March 2023).
4. Western Wind and Solar Integration Study. Available online: https://www.nrel.gov/grid/wwsis.html (accessed on 19 February 2023).
5. On the Performance of Support for Electricity from Renewable Sources Granted by Means of Tendering Procedures in the Union. Available online: https://eur-lex.europa.eu/legal-content/EN/TXT/?uri=CELEX:52022DC0638 (accessed on 5 February 2023).
6. On Amendments to Certain Acts of the Government of the Russian Federation on the Promotion of the Use of Renewable Energy Sources in the Retail Electricity Markets. Available online: http://government.ru/docs/all/94600/ (accessed on 6 February 2023).
7. Bhatt, U.S.; Carreras, B.A.; Barredo, J.M.R.; Newman, D.E.; Collet, P.; Gomila, D. The Potential Impact of Climate Change on the Efficiency and Reliability of Solar, Hydro, and Wind Energy Sources. *Land* **2022**, *11*, 1275. [CrossRef]
8. Solaun, K.; Cerdá, E. Climate change impacts on renewable energy generation. A review of quantitative projections. *Renew. Sust. Energ. Rev.* **2019**, *116*, 109415. [CrossRef]

9. Yu, M.; Wang, B.; Zhang, L.-L.; Chen, X. Wind speed forecasting based on EEMD and ARIMA. In Proceedings of the Chinese Automation Congress (CAC), Wuhan, China, 27–29 November 2015.
10. Qiao, H.; Chalermyanont, K.; Duangsoithong, R. Hour-Ahead Power Load Demand Time Series Forecasting Using Four Methods in Three Cases. In Proceedings of the 16th International Conference on Electrical Engineering/Electronics, Computer, Telecommunications and Information Technology (ECTI-CON), Pattaya, Thailand, 10–13 July 2019.
11. Cavalcante, L.; Bessa, R.J. Solar power forecasting with sparse vector autoregression structures. In Proceedings of the 2017 IEEE Manchester PowerTech, Manchester, UK, 18–22 June 2017.
12. Dowell, J.; Pinson, P. Very-Short-Term Probabilistic Wind Power Forecasts by Sparse Vector Autoregression. *IEEE Trans. Smart Grid.* **2015**, *7*, 763–770. [CrossRef]
13. Atique, S.; Noureen, S.; Roy, V.; Bayne, S.; MaCFie, J. Time series forecasting of total daily solar energy generation: A comparative analysis between ARIMA and machine learning techniques. In Proceedings of the IEEE Green Technologies Conference (GreenTech), Oklahoma City, OK, USA, 1–3 April 2020.
14. Hou, Z.J.; Etingov, P.V.; Makarov, Y.V.; Samaan, N.A. Uncertainty reduction in power generation forecast using coupled wavelet-ARIMA. In Proceedings of the IEEE PES General Meeting | Conference & Exposition, National Harbor, MD, USA, 27–31 July 2014.
15. Khalyasmaa, A.; Eroshenko, S.; Bramm, A.; Tran, D.C.; Chakravarthi, T.P.; Hariprakash, R. Strategic planning of renewable energy sources implementation following the country-wide goals of energy sector development. In Proceedings of the 2020 International Conference on Smart Technologies in Computing, Electrical and Electronics (ICSTCEE), Bengaluru, India, 9–10 October 2020.
16. Khalyasmaa, A.; Eroshenko, S.; Bramm, A.; Chakravarthi, T.P.; Hariprakash, R. Microgrid development for remote residential customers power supply. In Proceedings of the 2020 International Conference on Smart Technologies in Computing, Electrical and Electronics (ICSTCEE), Bengaluru, India, 9–10 October 2020.
17. Jurj, D.I.; Micu, D.D.; Muresan, A. Overview of electrical energy forecasting methods and models in renewable energy. In Proceedings of the 2018 International Conference and Exposition on Electrical and Power Engineering (EPE), Iasi, Romania, 18–19 October 2018.
18. Kim, J.H.; Munoz, P.A.J.; Sengupta, M.; Yang, J.; Dudhia, J.; Alessandrini, S.; Xie, Y. The WRF-Solar Ensemble Prediction System to Provide Solar Irradiance Probabilistic Forecasts. *IEEE J. Photovolt.* **2022**, *12*, 141–144. [CrossRef]
19. Jønler, J.F.; Lottrup, F.B.; Berg, B.; Zhang, D.; Chen, K. Probabilistic Forecasts of Global Horizontal Irradiance for Solar Systems. *IEEE Sens. Lett.* **2023**, *7*, 7000104. [CrossRef]
20. Jang, H.S.; Bae, K.Y.; Park, H.S.; Sung, D.K. Solar power prediction based on satellite images and support vector machine. *IEEE Trans. Sustain. Energy* **2016**, *7*, 1255–1263. [CrossRef]
21. Huang, Y.; Lu, J.; Liu, C.; Xu, X.; Wang, W.; Zhou, X. Comparative study of power forecasting methods for PV stations. In Proceedings of the 2010 International Conference on Power System Technology, Hangzhou, China, 24–28 October 2010.
22. Khalyasmaa, A.; Eroshenko, S.; Tran, D.C. Very-short term forecasting of photovoltaic plants generation based on meteorological data from open sources using machine learning. In Proceedings of the 2020 International Conference on Smart Technologies in Computing, Electrical and Electronics (ICSTCEE), Bengaluru, India, 9–10 October 2020.
23. Mutavhatsindi, T.; Sigauke, C.; Mbuvha, R. Forecasting Hourly Global Horizontal Solar Irradiance in South Africa Using Machine Learning Models. *IEEE Access* **2020**, *8*, 198872–198885. [CrossRef]
24. Ahmadi, A.; Nabipour, M.; Ivatloo, B.M.; Amani, A.M.; Rho, S.; Piran, M.J. Long-Term Wind Power Forecasting Using Tree-Based Learning Algorithms. *IEEE Access* **2020**, *8*, 151511–151522. [CrossRef]
25. Wang, K.; Zhang, Y.; Lin, F.; Wang, J.; Zhu, M. Nonparametric Probabilistic Forecasting for Wind Power Generation Using Quadratic Spline Quantile Function and Autoregressive Recurrent Neural Network. *IEEE Trans. Sustain. Energy* **2022**, *13*, 1930–1943. [CrossRef]
26. Mohamed, M.; Mahmood, F.E.; Abd, M.A.; Chandra, A.; Singh, B. Dynamic Forecasting of Solar Energy Microgrid Systems Using Feature Engineering. *IEEE Trans. Ind. Appl.* **2022**, *58*, 7857–7869. [CrossRef]
27. Rinne, H. *The Weibull Distribution: A Handbook*, 1st ed.; CRC Press: London, UK, 2008; pp. 98–188.
28. Malakar, S.; Ghosh, M.; Bhowmik, S. A GA based hierarchical feature selection approach for handwritten word recognition. *Neural. Comput. Appl.* **2020**, *32*, 2533–2552. [CrossRef]
29. Rahman, C.M.; Rashid, T.A.; Alsadoon, A. A survey on dragonfly algorithm and its applications in engineering. *Evol. Intel.* **2023**, *16*, 1–21. [CrossRef]
30. Matrenin, P.; Myasnichenko, V.; Sdobnyakov, N.; Sokolov, D.; Fidanova, S.; Kirilov, L.; Mikhov, R. Generalized swarm intelligence algorithms with domain-specific heuristics. *IAES* **2021**, *10*, 157–165. [CrossRef]
31. Shukla, N.K.; Srivastava, R.; Mirjalili, S. A Hybrid Dragonfly Algorithm for Efficiency Optimization of Induction Motors. *Sensors* **2022**, *22*, 2594. [CrossRef] [PubMed]
32. Dalia, Y.; Thanikanti, S.B.; Seyedali, M.; Rajasekar, N.; Mohamed, A.E. A novel objective function with artificial ecosystem-based optimization for relieving the mismatching power loss of large-scale photovoltaic array. *Energy Convers. Manag.* **2020**, *225*, 113385.
33. Ridha, H.M.; Hizam, H.; Mirjalili, S.; Othman, M.L.; Ya'acob, M.E.; Ahmadipour, M. Innovative hybridization of the two-archive and PROMETHEE-II triple-objective and multi-criterion decision making for optimum configuration of the hybrid renewable energy system. *Appl. Energy* **2023**, *341*, 121117. [CrossRef]
34. El-Sayed, M.E.; Seyedali, M.; Nima, K.; Abdelaziz, A.A.; Marwa, M.E.; El-Said, M.; Abdelhameed, I. Feature selection in wind speed forecasting systems based on meta-heuristic optimization. *PLoS ONE* **2023**, *18*, e0278491.

35. Qaraad, M.; Amjad, S.; Hussein, N.K.; Badawy, M.; Mirjalili, B.; Elhosseini, M.A. Photovoltaic parameter estimation using improved moth flame algorithms with local escape operators. *Comput. Electr. Eng.* **2023**, *106*, 108603. [CrossRef]
36. Nasa Power. Available online: https://power.larc.nasa.gov/docs/services/api/ (accessed on 15 February 2023).
37. Jiang, X.; Li, J.; Lu, Y.; Tian, G. Design of Reverse Logistics Network for Remanufacturing Waste Machine Tools Based on Multi-Objective Gray Wolf Optimization Algorithm. *IEEE Access* **2020**, *8*, 141046–141056. [CrossRef]
38. Zhang, W.; Zhang, S.; Wu, F.; Wang, Y. Path Planning of UAV Based on Improved Adaptive Grey Wolf Optimization Algorithm. *IEEE Access* **2021**, *9*, 89400–89411. [CrossRef]
39. Guo, M.W.; Wang, J.S.; Zhu, L.F.; Guo, S.S.; Xie, W. An Improved Grey Wolf Optimizer Based on Tracking and Seeking Modes to Solve Function Optimization Problems. *IEEE Access* **2020**, *8*, 69861–69893. [CrossRef]
40. Mohanty, S.; Subudhi, B.; Ray, P.K. A New MPPT Design Using Grey Wolf Optimization Technique for Photovoltaic System Under Partial Shading Conditions. *IEEE Trans. Sustain. Energy* **2016**, *7*, 181–188. [CrossRef]
41. Yousri, D.; Thanikanti, S.B.; Balasubramanian, K.; Osama, A.; Fathy, A. Multi-Objective Grey Wolf Optimizer for Optimal Design of Switching Matrix for Shaded PV array Dynamic Reconfiguration. *IEEE Access* **2020**, *8*, 159931–159946. [CrossRef]
42. Bramm, A.; Eroshenko, S.; Khalyasmaa, A. Effect of Data Preprocessing on the Forecasting Accuracy of Solar Power Plant. In Proceedings of the 2021 XVIII International Scientific Technical Conference Alternating Current Electric Drives (ACED), Ekaterinburg, Russia, 24–27 May 2021.
43. Prema, V.; Bhaskar, M.S.; Almakhles, D.; Gowtham, N.; Rao, K.U. Critical Review of Data, Models and Performance Metrics for Wind and Solar Power Forecast. *IEEE Access* **2022**, *10*, 667–688. [CrossRef]